Article

Absolute Rates of Hole Transfer in DNA

Kittusamy Senthilkumar, Ferdinand C. Grozema, Clia Fonseca Guerra, F. Matthias Bickelhaupt, Frederick D. Lewis, Yuri A. Berlin, Mark A. Ratner, and Laurens D. A. Siebbeles

J. Am. Chem. Soc., **2005**, 127 (42), 14894-14903• DOI: 10.1021/ja054257e • Publication Date (Web): 24 September 2005

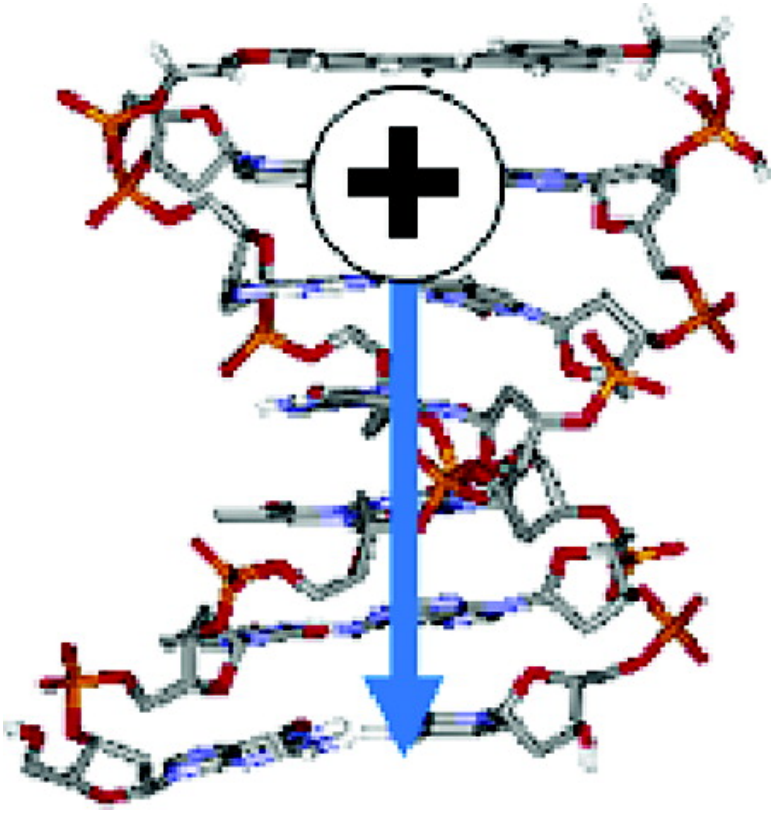

J|A|C|S
ARTICLES
Published on Web 09/24/2005

Absolute Rates of Hole Transfer in DNA

Kittusamy Senthilkumar,[‡] Ferdinand C. Grozema,[‡] Célia Fonseca Guerra,[#] F. Matthias Bickelhaupt,[#] Frederick D. Lewis,[†] Yuri A. Berlin,[†] Mark A. Ratner,[†] and Laurens D. A. Siebbeles*,[‡]

Contribution from the Opto-Electronic Materials Section, DelftChemTech, Delft University of Technology, Mekelweg 15, 2629 JB Delft, The Netherlands, Afdeling Theoretische Chemie, Scheikundig Laboratorium der Vrije Universiteit, De Boelelaan 1083, NL-1081 HV Amsterdam, The Netherlands, and Department of Chemistry, Northwestern University, Evanston, Illinois 60208-3113

Received June 28, 2005; E-mail: l.d.a.siebbeles@tnw.tudelft.nl

Abstract: Absolute rates of hole transfer between guanine nucleobases separated by one or two A:T base pairs in stilbenedicarboxamide-linked DNA hairpins were obtained by improved kinetic analysis of experimental data. The charge-transfer rates in four different DNA sequences were calculated using a density-functional-based tight-binding model and a semiclassical superexchange model. Site energies and charge-transfer integrals were calculated directly as the diagonal and off-diagonal matrix elements of the Kohn−Sham Hamiltonian, respectively, for all possible combinations of nucleobases. Taking into account the Coulomb interaction between the negative charge on the stilbenedicarboxamide linker and the hole on the DNA strand as well as effects of base pair twisting, the relative order of the experimental rates for hole transfer in different hairpins could be reproduced by tight-binding calculations. To reproduce quantitatively the absolute values of the measured rate constants, the effect of the reorganization energy was taken into account within the semiclassical superexchange model for charge transfer. The experimental rates could be reproduced with reorganization energies near 1 eV. The quantum chemical data obtained were used to discuss charge carrier mobility and hole-transport equilibria in DNA.

Introduction

The mechanism of charge migration through DNA attracts a great deal of interest because of its relevance to oxidative strand cleavage,[1,2] to the development of nanoelectronics[3−6] and biosensor devices,[7−12] and to electrochemical sequencing techniques.[13−15] With a few exceptions,[16−23] experimental and theoretical results obtained so far refer to the motion of positive charges (holes) rather than to the migration of excess electrons. This process has been probed using both steady-state and time-resolved methods.

Steady-state methods usually exploit measurements of damage ratios or the conductivity of DNA molecules with different length and base pair arrangement; for recent reviews see, e.g., refs 24−28. The outcome of such measurements includes data on the efficiency of the hole-transport process through DNA and information about the distance over which charges can migrate through a stack of base pairs.

Theoretical analysis of the steady-state experiments relies on the mechanistic picture of charge migration in DNA. There is

[‡] Delft University of Technology.
[#] Vrije Universiteit.
[†] Northwestern University.

(1) Armitage, B. *Chem. Rev.* **1998**, *98*, 1171−1200.
(2) Burrow, C. J.; Muller, J. G. *Chem. Rev.* **1998**, *98*, 1109−1151.
(3) Ratner, M. A.; Jortner, J. *Molecular electronics*; Blackwell: Oxford, 1997.
(4) Bhalla, V.; Bajpai, R. P.; Bharadwaj, L. M. *EMBO Rep.* **2003**, *4*, 442−445.
(5) Tabata, H.; Cai, L. T.; Gu, J. H.; Tanaka, S.; Otsuka, Y.; Sacho, Y.; Taniguchi, M.; Kawai, T. *Synth. Met.* **2003**, *133*, 469−472.
(6) Di Ventra, M.; Zwolak, M. In *Encyclopedia of Nanoscience and Nanotechnology*; Nalwa, H. S., Ed.; American Scientific Publishers: Stevenson Ranch, CA, 2004.
(7) Hartwich, G.; Caruana, D. J.; de Lumley-Woodyear, T.; Wu, Y. B.; Campbell, C. N.; Heller, A. *J. Am. Chem. Soc.* **1999**, *121*, 10803−10812.
(8) Lisdat, F.; Ge, B.; Scheller, F. W. *Electrochem. Commun.* **1999**, *1*, 65−68.
(9) Park, S. J.; Lazarides, A. A.; Mirkin, C. A.; Brazis, P. W.; Kannewurf, C. R.; Letsinger, R. L. *Angew. Chem., Int. Ed.* **2000**, *39*, 3845−3848.
(10) Boon, E. M.; Ceres, D. M.; Drummond, T. G.; Hill, M. G.; Barton, J. K. *Nat. Biotechnol.* **2000**, *18*, 1096−1100.
(11) Niemeyer, C. M. *Angew. Chem., Int. Ed.* **2001**, *40*, 4128−4158.
(12) Park, S.-J.; Taton, T. A.; Mirkin, C. A. *Science* **2002**, *295*, 1503−1506.
(13) Marshall, A.; Hodgson, J. *Nat. Biotechnol.* **1998**, *16*, 27−31.
(14) Kelley, S. O.; Jackson, N. M.; Hill, M. G.; Barton, J. K. *Angew. Chem., Int. Ed.* **1999**, *38*, 941−945.
(15) Lisdat, F.; Ge, B.; Scheller, F. W. *Electrochem. Commun.* **1999**, *1*, 65−68.
(16) Ito, T.; Rakita, S. E. *J. Am. Chem. Soc.* **2003**, *125*, 11480−11481.
(17) Behrens, C.; Ober, M.; Carell, T. *Eur. J. Org. Chem.* **2002**, *19*, 3281−3289.
(18) Behrens, C.; Burgdorf, L. T.; Schwögler, A.; Carell, T. *Angew. Chem., Int. Ed.* **2002**, *41*, 1763−1766.
(19) Behrens, C.; Carell, T. *Chem. Commun.* **2003**, *14*, 1632−1633.
(20) Breeger, S.; Hennecke, U.; Carell, T. *J. Am. Chem. Soc.* **2004**, *126*, 1302−1303.
(21) Wagenknecht, H. A. *Angew. Chem., Int. Ed.* **2003**, *42*, 2454−2460.
(22) Kaden, P.; Mayer-Enthart, E.; Trifonov, A.; Foebog, T.; Wagenknecht, H. A. *Angew. Chem., Int. Ed.* **2005**, *44*, 1637−1639.
(23) Razskazovskii, Y.; Swarts, S. G.; Falcone, J. M.; Taylor, C.; Sevilla, M. D. *J. Phys. Chem. B* **1997**, *101*, 1460−1467.
(24) Giese, B. *Acc. Chem. Res.* **2000**, *33*, 631−636.
(25) Schuster, G. B. *Acc. Chem. Res.* **2000**, *33*, 253−260.
(26) Treadway, C. R.; Hill, M. G.; Barton, J. K. *Chem. Phys.* **2002**, *281*, 409−428.
(27) O'Neill, M. A.; Barton, J. K. *Top. Curr. Chem.* **2004**, *236*, 67−115.
(28) Endres, R. G.; Cox, D. L.; Singh, R. R. P. *Rev. Mod. Phys.* **2004**, *76*, 195−213.

10.1021/ja054257e CCC: $30.25

general agreement that holes move through the stack of base pairs inside the double helix by a series of short hops, although the nature of these hopes remains the subject of intensive discussions. The latter issue is closely related to the problem of charge localization/delocalization in the stack of nucleobases.

If a hole is able to form a polaron due to self-trapping by a distortion of the base pair stack[29,30] and in the local surrounding water molecules[31] and counterions to the phosphate anions of the backbone,[32] the excess positive charge can be extended over several bases. In this case, hole transport in DNA is expected to proceed via sequential phonon-assisted polaron hopping.[29] The latter process has been treated theoretically within the adiabatic models proposed in refs 30 and 33. However, recent calculations reported by Voityuk[34] indicate that polar surroundings essentially suppress charge delocalization in DNA, and hole states are localized on individual guanines (G) even in sequences containing only adjacent guanine:cytosine (G:C) base pairs. This result does not support the earlier conclusion of Basko and Conwell[35] that the hole charge can be spread over five or more G:C sites, leading to polaron formation in such sequences. Another effect resulting in the hole confinement to a single base pair is internal (structural) reorganization of nucleobases caused by an excess charge. According to Olofsson and Larsson,[36] spatially well-localized hole states are energetically stabilized due to the internal reorganization of nucleobases, thus reinforcing the hole localization to a single base pair.

Unlike polaron hopping, the motion of a positive charge confined to a single base pair is viewed as a series of hops between G sites. Within this mechanistic picture, each single G is a stepping stone for hole transport,[37−43] since this base has the lowest oxidation potential among the four native nucleobases. Once a hole is generated on a particular G site, it can be transferred to another G separated by a bridge of adenine:thymine (A:T) base pairs. As a consequence, the transport process of a hole along a sequence consisting of G:C linked by A:T bridges of different lengths can be considered as a series of elementary steps of variable lengths determined by the distance between neighboring G's. In this mechanistic picture of variable-range hopping transport, each elementary step proceeds via tunneling or by thermal activation. The tunneling channel is dominant for bridges with a length of at most four A:T base pairs, while the mechanism of thermal activation becomes operative for longer bridges.[44−47]

An obvious advantage of this variable-range hopping model[37,40,43,46,48,49] is the possibility to describe phenomenologically both sequence and distance dependencies for the efficiency of hole transfer through various sequences of Watson−Crick base pairs. Such a possibility was demonstrated[43] for sequences studied experimentally by Giese et al.,[44,50,51] by Nakatani et al.,[52] and by Schuster and co-workers.[29,53] The only phenomenological parameter needed for the description of the observed sequence and distance dependencies within the framework of the variable-range hopping model involves experimental data[44,50,54] about relative rates for individual, local hopping steps of different lengths. Knowledge of the relative rates also enables one to use the variable-range hopping model for reasonable evaluation of the distance scale for the propagation of a positive charge in DNA duplexes.[39,43] The significance of relative but not absolute rates for theoretical analysis of steady-state experiments is a direct consequence of two competitive decay channels existing for a positive charge at each step of the transport process, namely hole transfer between nearest-neighbor G sites through the AT bridge and irreversible side reaction of the cation G^+ with water.

Knowledge of relative hopping rates, however, is insufficient to determine how fast a hole generated in DNA can be transferred over a certain distance. To address this issue, absolute rates of different hopping steps should be obtained. Experimentally this has been done by performing time-resolved measurements on DNA containing different charge donor and acceptor moieties.[55−62] The experiments on DNA hairpins are of particular importance,[56−59] since only for these systems do guanine nucleobases serve as hole donor and acceptor, while in other time-resolved experiments other molecules distinct from DNA nucleobases are used for this purpose.

The aim of the current work is two-fold. The first objective is to provide the values of the parameters needed to describe hole hopping between G's. These include charge-transfer integrals (also referred to as electronic coupling elements or hopping matrix elements) and site energies (the energy of a hole when it is localized at a particular nucleobase). The second objective is to use these parameters for theoretical evaluation of absolute rates for hole transfer between G nucleobases

(29) Henderson, P. T.; Jones, D.; Hampikian, G.; Kan, Y.; Schuster, G. B. *Proc. Natl. Acad. Sci. U.S.A.* **1999**, *96*, 8353−8358.
(30) Conwell, E. M. *Top. Curr. Chem.* **2004**, *237*, 73−101.
(31) Conwell, E. M. *Proc. Natl. Acad. Sci. U.S.A.* **2005**, *102*, 8795−8799.
(32) Barnett, R. N.; Cleveland, C. L.; Joy, A.; Landman, U.; Schuster, G. B. *Science* **2001**, *294*, 567−571.
(33) Liu, C.-S.; Hernandez, R.; Schuster, G. B. *J. Am. Chem. Soc.* **2004**, *126*, 2877−2844.
(34) Voityuk, A. A. *J. Chem. Phys.* **2005**, *122*, 204904.
(35) Basko, D. M.; Conwell, E. M. *Phys. Rev. Lett.* **2002**, *88*, 098102.
(36) Olofsson, J.; Larsson, S. *J. Phys. Chem. B* **2001**, *105*, 10398−10406.
(37) Jortner, J.; Bixon, M.; Langenbacher, T.; Michel-Beyerle, M. E. *Proc. Natl. Acad. Sci. U.S.A.* **1998**, *95*, 12759−12765.
(38) Ratner, M. A. *Nature* **1999**, *397*, 480−481.
(39) Bixon, M.; Giese, B.; Wessely, S.; Langenbacher, T.; Michel-Beyerle, M. E.; Jortner, J. *Proc. Natl. Acad. Sci. U.S.A.* **1999**, *96*, 11713−11716.
(40) Berlin, Y. A.; Burin, A. L.; Ratner, M. A. *J. Phys. Chem. A* **2000**, *104*, 443−445.
(41) Grozema, F. C.; Berlin, Y. A.; Siebbeles, L. D. A. *Int. J. Quantum Chem.* **1999**, *75*, 1009−1016.
(42) Grozema, F. C.; Berlin, Y. A.; Siebbeles, L. D. A. *J. Am. Chem. Soc.* **2000**, *122*, 10903−10909.
(43) Berlin, Y. A.; Burin, A. L.; Ratner, M. A. *J. Am. Chem. Soc.* **2001**, *123*, 260−268.
(44) Giese, B.; Amaudrut, J.; Köhler, A.-K.; Spermann, M.; Wessely, S. *Nature* **2001**, *412*, 318−320.
(45) Berlin, Y. A.; Burin, A. L.; Ratner, M. A. *Chem. Phys.* **2002**, *275*, 61−74.
(46) Bixon, M.; Jortner, J. *Chem. Phys.* **2002**, *281*, 393−408.
(47) Shimazaki, T.; Asai, Y.; Yamashita, K. *J. Phys. Chem. B* **2005**, *109*, 1295−1303.
(48) Berlin, Y. A.; Kurnikov, I. V.; Beratan, D.; Ratner, M. A.; Burin, A. L. *Top. Curr. Chem.* **2004**, *237*, 1−36.
(49) Bicout, D. J.; Kats, E. *Phys. Lett. A* **2002**, *300*, 479−484.
(50) Meggers, E.; Michel-Beyerle, M. E.; Giese, B. *J. Am. Chem. Soc.* **1998**, *120*, 12950−12915.
(51) Giese, B.; Wessely, S.; Spormann, M.; Lindemann, U.; Meggers, E.; Michel-Beyerle, M. E. *Angew. Chem., Int. Ed.* **1999**, *38*, 996−998.
(52) Nakatani, K.; Dohno, C.; Saito, I. *J. Am. Chem. Soc.* **1999**, *121*, 10854−10855.
(53) Ly, D.; Sanii, L.; Schuster, G. B. *J. Am. Chem. Soc.* **1999**, *121*, 9400−9410.
(54) Giese, B. *Curr. Opin. Chem. Biol.* **2002**, *6*, 612−618.
(55) Wan, C.; Fiebig, T.; Kelley, S. O.; Treadway, C. R.; Barton, J. K.; Zewail, A. H. *Proc. Natl. Acad. Sci. U.S.A.* **1999**, *96*, 6014−6019.
(56) Lewis, F. D.; Liu, X.; Liu, J.; Miller, S. E.; Hayes, R. T.; Waslelewski, M. R. *Nature* **2000**, *406*, 51−53.
(57) Lewis, F. D.; Letsinger, R. L.; Wasielewski, M. R. *Acc. Chem. Res.* **2001**, *34*, 159−170.
(58) Lewis, F. D.; Zuo, X.; Liu, J.; Hayes, R. T.; Wasielewski, M. R. *J. Am. Chem. Soc.* **2002**, *124*, 4568−4569.
(59) Lewis, F. D.; Liu, J.; Zuo, X.; Hayes, R. T.; Wasielewski, M. R. *J. Am. Chem. Soc.* **2003**, *125*, 4850−4861.
(60) Hess, S.; Götz, M.; Davis, W. B.; Michel-Beyerle, M.-E. *J. Am. Chem. Soc.* **2001**, *123*, 10046−10055.
(61) Takada, T.; Kawai, K.; Tojo, S.; Majima, T. *J. Phys. Chem. B* **2003**, *107*, 14052−14057.
(62) Takada, T.; Kawai, K.; Cai, X.; Sugimoto, A.; Fujitsuka, M.; Majima, T. *J. Am. Chem. Soc.* **2004**, *126*, 1125−1129.

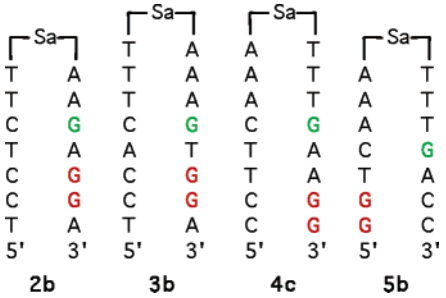

Figure 1. DNA hairpins studied in the present work.

separated by A:T base pairs. The calculated parameters are also utilized to gain deeper insight into the mobility of holes and charge-transport equilibria in DNA.

The calculated results are compared with time-resolved measurements on DNA sequences with a stilbenedicarboxamide (**Sa**) electron acceptor.[58,59] The structures[63,64] considered in the present work are schematically shown in Figure 1. The annotation of the sequences is taken from ref 59.

The first objective of this work was achieved using Kohn−Sham density functional theory (DFT)[65] as implemented in the Amsterdam Density Functional (ADF) theory program.[66] With this program, the orbitals of a stack of nucleobase pairs can be expressed in terms of the molecular orbitals on the individual nucleobases.[67] The spatial overlap integrals belong to the standard output of the ADF program, while the charge-transfer integrals and site energies involved in hole transport are directly obtained as the off-diagonal and diagonal matrix elements of the Kohn−Sham Hamiltonian multiplied by −1, i.e., $-\mathbf{h}_{KS}$. This methodology has been applied earlier to describe charge-transport properties of stacks of triphenylene molecules[68] and site-selective photo-oxidation in DNA.[67]

The second objective, i.e., calculations of the rate of hole transfer in DNA hairpins, was realized within the tight-binding[41,42,69] approach and semiclassical superexchange[46,70] model. Comparison of calculated and experimental rate constants shows that the rate of hole transfer is strongly affected by the reorganization energy and by the Coulomb interaction between the stilbenedicarboxamide anion and the hole generated in the hairpins studied.

Kinetic Analysis of Experimental Data

Absolute rates for different steps of hole transport in DNA hairpins (see Figure 1) can be obtained from the time-resolved measurements described in refs 58 and 59. The experimental results suggest that photoexcitation of **Sa** initially leads to the formation of the anion radical $\mathbf{Sa}^{-\bullet}$ and a hole on the G site nearest to **Sa**. The hole generated on this proximal G is able either to recombine with $\mathbf{Sa}^{-\bullet}$ with a rate constant k_{cr} or to jump to a distal GG doublet with a rate constant k_t. The latter process leads to the formation of $(GG)^+$ but does not terminate the motion of positive charges, since a hole can be back-transferred to the primary G site with a rate constant k_{-t}.

In the experiments described in refs 58 and 59, the transient optical absorption of the anion radical $\mathbf{Sa}^{-\bullet}$ was monitored as a function of time. The population of these anions is equal to that of holes on the DNA sequence. The transient absorption is thus proportional to the total population of holes on all G sites on the DNA hairpin studied. Therefore, to obtain information about the rate constants for each hopping step from the measured transient absorption, an expression describing the time evolution of the hole population is needed.

To derive the expression required, it is useful to recognize that the photoinduced generation of $\mathbf{Sa}^{-\bullet}$ and the hole on the proximal G is much faster than all other charge-transport steps mentioned above.[57−59] It can thus be assumed that the hole is initially localized on the proximal G site nearest to $\mathbf{Sa}^{-\bullet}$. Then the kinetic equations describing the populations X and Y of holes on this proximal G and on the distal GG doublet are given by

$$\frac{dX}{dt} = -k_t X - k_{cr} X + k_{-t} Y, \quad \frac{dY}{dt} = k_t X - k_{-t} Y$$

The solution of these equations, which satisfies the initial conditions $X(t{=}0) = 1$ and $Y(t{=}0) = 0$, can be written as

$$X(t) = \frac{X(t{=}0)}{\lambda_2}\left[\left(k_{-t} - \frac{\lambda_1 - \lambda_2}{2}\right)\exp\left(-\frac{1}{2}(\lambda_1 - \lambda_2)t\right) + \left(\frac{\lambda_1 + \lambda_2}{2} - k_{-t}\right)\exp\left(-\frac{1}{2}(\lambda_1 + \lambda_2)t\right)\right] \quad (1a)$$

$$Y(t) = \frac{k_t}{\lambda_2} X(t{=}0)\left[\exp\left(-\frac{1}{2}(\lambda_1 - \lambda_2)t\right) - \exp\left(-\frac{1}{2}(\lambda_1 + \lambda_2)t\right)\right] \quad (1b)$$

with $\lambda_1 = k_{cr} + k_t + k_{-t}$ and $\lambda_2 = (\lambda_1^2 - 4k_{cr}k_{-t})^{1/2}$.

The rate constants k_{cr}, k_t, and k_{-t} can be obtained from a fit of the sum of eqs 1a and 1b to the measured transient optical absorption. The results for sequences **2b** and **3b** are given in Figure 2. It can be seen that the experimental data can be very well reproduced by the kinetic scheme described above. The values obtained for the rate constants in the sequences shown in Figure 1 are presented in Table 1. The uncertainty in the rate constants obtained from the fits is less than 20%.

It should be noted that the present results for the rate constants differ from those reported earlier.[58,59] This is due to the fact that instead of using the exact expressions for $X(t)$ and $Y(t)$, the transient absorption was described in the work of refs 58 and 59 as a sum of two exponentials with adjustable amplitudes. Obviously, this postulated fitting function yields values of rate constants distinct from those obtained by using eq 1. The most significant differences were found for sequences **2b** and **3b**. In particular, as can be seen from Table 1 and the data of refs 58 and 59, the rate constant for charge recombination, k_{cr}, in sequence **2b** obtained by using eq 1 is about one-fourth the value of this rate constant found with the postulated fitting function. In addition, the rate constant, k_t, for forward hole

(63) Lewis, F. D.; Liu, X. Y.; Wu, Y. S.; Miller, S. E.; Wasielewski, M. R.; Letsinger, R. L.; Sanishvili, R.; Joachimiak, A.; Tereshko, V.; Egli, M. *J. Am. Chem. Soc.* **1999**, *121*, 9905−9906.
(64) Lewis, F. D.; Letsinger, R. L.; Wasielewski, M. R.; Egli, M. *Biophys. J.* **2000**, *78*, 139A−139A.
(65) Bickelhaupt, F. M.; Baerends, E. J. In *Reviews on Computational Chemistry*; Lipkowitz, K. B., Boyd, D. B., Eds.; Wiley-VCH: New York, 2000; Vol. 15, pp 1−86.
(66) Te Velde, G.; Bickelhaupt, F. M.; Baerends, E. J.; Fonseca Guerra, C.; Van Gisbergen, S. J. A.; Snijders, J. G.; Ziegler, T. *J. Comput. Chem.* **2001**, *22*, 931−967.
(67) Senthilkumar, K.; Grozema, F. C.; Guerra, C. F.; Bickelhaupt, F. M.; Siebbeles, L. D. A. *J. Am. Chem. Soc.* **2003**, *125*, 13658−13659.
(68) Senthilkumar, K.; Grozema, F. C.; Bickelhaupt, F. M.; Siebbeles, L. D. A. *J. Chem. Phys.* **2003**, *119*, 9809−9817.
(69) Grozema, F. C.; Siebbeles, L. D. A.; Berlin, Y. A.; Ratner, M. A. *ChemPhysChem* **2002**, *6*, 536−539.
(70) Bixon, M.; Jortner, J. *Adv. Chem. Phys.* **1999**, *106*, 35−208.

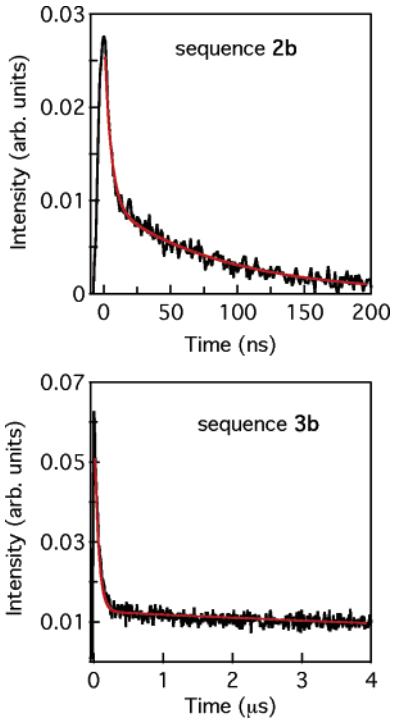

Figure 2. Measured decay of the transient absorption (black) and fits of the sum of eqs 1a and 1b (red) for hairpins **2b** and **3b**. Note the different time scales.

Table 1. Rate Constants, Electronic Couplings, and Reorganization Energies in DNA Hairpins

	rate constants[a] (s^{-1})			electronic coupling[b] (eV)		reorganization energies[c] (eV)	
sequence	$10^{-7}\ k_{cr}$	$10^{-7}\ k_t$	$10^{-7}\ k_{-t}$	$10^3\ V_t$	$10^3\ V_{-t}$	λ_t	λ_{-t}
2b	14.2	6.0	1.7	8.68	8.71	1.00	1.13
3b	1.4	0.33	0.0083	2.15	1.65	1.46	0.76
4c	0.37	0.048	0.0024	0.49	0.32	1.09	0.93
5b	0.37	0.09	0.009	0.42	0.27	1.00	0.78

[a] Obtained by fitting eq 1 to the experimental data of refs 58 and 59. [b] Calculated from eqs 7b and 8 as explained in the text. [c] Values needed to reproduce the experimental rate constants using the Marcus equation (eq 7).

transfer in sequence **3b** is about an order of magnitude higher than reported earlier.[58,59]

Comparison of the rate constants for hole transfer in sequences **2b** and **3b** shows that hole transfer between the proximal G site and the distal GG doublet via an intervening adenine (A) is much faster than via thymine (T) on the same strand. The rate constant for forward hole transfer decreases significantly upon introduction of an additional AT base pair, cf. sequences **2b** and **4c**. The results for sequences **2b** and **5b** show that intrastrand charge transfer between G sites is much faster than analogous interstrand processes.

Charge-Transfer Integrals and Site Energies

1. Computational Methodology. In the present work, charge transport through DNA is described within the framework of a tight-binding method[41,42,48,69] and superexchange model.[46,48,70] Both approaches are based on a Hamiltonian given by

$$H = \sum_i \epsilon_i(R(t)) a_i^+ a_i + \sum_{\substack{i,j \\ i \neq j}} J_{i,j}(R(t)) a_i^+ a_j \qquad (2)$$

In eq 2, a_i^+ and a_i are the creation and annihilation operators of a charge at the ith nucleobase, $\epsilon_i(R(t)) = \langle \varphi_i | H | \varphi_i \rangle$ is the site energy of the charge, and $J_{i,j}(R(t)) = \langle \varphi_i | H | \varphi_j \rangle$ is the charge-transfer integral involving molecular orbitals, φ_i, on the nucleobases i and j. In eq 2, both the site energies and the charge-transfer integrals depend on the intramolecular and intermolecular geometric degrees of freedom, which may fluctuate in time and are collectively denoted as $R(t)$. For a complete description of the dynamics of a charge carrier, the kinetic energy due to nuclear motions must be added to eq 1, as has been done in a previous study on the mobility of holes in DNA.[69]

The wave function of a hole can, to a good approximation, be written as a linear superposition of the highest occupied molecular orbitals (HOMOs) on the individual nucleobases. The HOMOs, φ_i, of individual nucleobases were calculated from DFT using the ADF program[66] with a basis set consisting of atomic orbitals. The site energies and charge-transfer integrals in eq 2 were obtained by utilizing a unique feature of the ADF program, namely the possibility to exploit the molecular orbitals, φ_i (fragment orbitals), as a basis set in calculations on a system consisting of two or more nucleobases. With the ADF program the eigenvector matrix **C** is obtained by solving the Kohn−Sham equation $\mathbf{h}_{KS}\mathbf{C} = \mathbf{SCE}$, with **E** the diagonal matrix containing the eigenvalues of the orbitals of the composite system consisting of two or more nucleobases. Note that the eigenvector matrix, **C**, and the overlap matrix, **S** ($S_{ij} = \langle \varphi_i | \varphi_j \rangle$), are defined in terms of the molecular orbitals, φ_i, on the individual nucleobases rather than in terms of the atomic orbitals. The standard output of the ADF program provides the overlap matrix, **S**, the eigenvector matrix, **C**, and the eigenvalue matrix, **E**. The matrix elements of the Kohn−Sham Hamiltonian, $\langle \varphi_i | h_{KS} | \varphi_j \rangle$, can readily be obtained by using the relation $\mathbf{h}_{KS} = \mathbf{SCEC}^{-1}$. This procedure allows direct calculations of the charge-transfer integrals, including their signs, without invoking the assumption of zero spatial overlap. Therefore, it is not necessary to apply an external electric field to bring the site energies of different nucleobases into resonance.[36,71−73] This distinguishes the present calculations from quantum chemical studies based on the energetic splitting of orbitals.[36,71−73] The most important advantage of the present method, however, is the possibility to calculate the site energies as $\epsilon_i = -\langle \varphi_i | h_{KS} | \varphi_i \rangle$, which cannot be obtained from the orbital splitting procedure.[74] Note that the sign of the matrix elements in eq 2 for a description of hole transport is opposite that of the corresponding matrix elements of $\mathbf{h}_{KS}$ involving the electronic orbitals of the missing electron.

The DFT calculations were performed with an atomic basis set of Slater-type orbitals (STOs) of triple-ζ quality including two sets of polarization functions on each atom (TZ2P basis set in ADF).[75] This type of orbitals gives a better description of the tails of the electron wave function as compared to Gaussian-type orbitals. Hence, they are more suitable for calculations of charge-transfer integrals, which are mainly determined by these tails. The asymptotically corrected exchange

(71) Voityuk, A. A.; Rosch, N.; Bixon, M.; Jortner, J. *J. Phys. Chem. B* **2000**, *104*, 9740−9745.
(72) Voityuk, A. A.; Jortner, J.; Bixon, M.; Rosch, N. *J. Chem. Phys.* **2001**, *114*, 5614−5620.
(73) Voityuk, A. A.; Rosch, N. *J. Chem. Phys.* **2002**, *117*, 5607−5620.
(74) Newton, M. D. *Chem. Rev.* **1991**, *91*, 767−792.
(75) Snijders, J. G.; Vernooijs, P.; Baerends, E. J. *At. Data Nucl. Data Tables* **1981**, *26*, 483−509.

Table 2. Site Energies (in eV) for Nucleobase B in 5′-XBY-3′ Triads (X, B, Y = G, A, C, and T)

Y	G	A	T	C	Y	G	A	T	C
GGY	7.890	8.040	8.290	8.310	GTY	9.111	9.308	9.533	9.557
AGY	7.900	8.060	8.320	8.341	ATY	9.130	9.370	9.586	9.578
CGY	7.957	8.115	8.361	8.383	CTY	9.268	9.451	9.662	9.701
TGY	7.965	8.124	8.380	8.407	TTY	9.273	9.499	9.699	9.705
GAY	8.343	8.487	8.712	8.716	GCY	9.446	9.637	9.870	9.857
AAY	8.376	8.558	8.799	8.763	ACY	9.441	9.630	9.867	9.851
CAY	8.438	8.584	8.793	8.800	CCY	9.490	9.667	9.917	9.882
TAY	8.434	8.630	8.858	8.810	TCY	9.499	9.679	9.925	9.895

correlation potential SAOP (statistical average of orbital potentials) was used in the DFT calculations.[76] As has been shown earlier,[67] this potential yields reliable results both for the relative ionization energies of isolated nucleobases and for the relative site energies of G nucleobases in DNA stacks.

The geometries of stacks of two or three base pairs were generated using the SCHNARP program with standard global helical parameters of B-form DNA.[77] The effect of flanking base pairs on the site energy for a particular nucleobase was taken into account by calculating the site energies for nucleobases in the middle of a stack of three base pairs. Charge-transfer integrals and spatial overlap matrix elements were calculated as a function of twist angle between two base pairs at a distance of 3.38 Å. The electronic effect of the sugar−phosphate backbone on the nucleobases was modeled by replacing the sugar−phosphate units with methyl groups. Inclusion of the sugar−phosphate backbone will not significantly affect the values of the charge-transfer integrals and site eneregies, since the HOMOs were found to be almost entirely (>96%) localized on the nucleobases, while the density on the methyl group was very small, in agreement with earlier findings.[78]

2. Results. The site energies involved in hole transport, which are defined as the diagonal matrix elements of the Kohn−Sham Hamiltonian (with inverted sign) involving the HOMOs on the nucleobases G, A, C, and T, are given in Table 2 for all possible combinations of flanking nucleobases at the 5′- and 3′-positions. The effect of the flanking nucleobase at the 5′-position on the site energies is much less pronounced than the effect of the nucleobase at the 3′-position. The site energy of G flanked by another G at the 3′-position is considerably lower than in cases where G is flanked by another nucleobase at the 3′-position. For all nucleobases, the site energy is smaller when G or A is present at the 3′-position than in cases where C or T is present the 3′-position. It is worth mentioning that the site energies do not always increase in the order G < A < C < T known for the hierarchy of the ionization energies of individual nucleobases.[79] For instance, the site energy of G in 5′-TGC-3′ is higher than the site energy of A in the sequence 5′-GAG-3′. Similar trends were obtained for the calculated ionization energies of base pair triplets in ref 80.

The charge-transfer and spatial overlap integrals for nucleobases within the Watson−Crick base pairs are $J = -0.085$ eV and $S = -0.006$ for G:C, while $J = -0.11$ eV and $S = -0.007$ for A:T. The values of J and S for all other combinations of nucleobases in neighboring base pairs are given in Table 3. Following the notation in ref 72, the nucleobases B_1 and B_2 (see Scheme 1) in one strand involved in intrastrand electronic coupling are symbolized in Table 3 as 5′-B_1B_2-3′. Similarly, the nucleobases b_1 and b_2 coupled within the other strand are denoted as 3′-b_1b_2-5′. As illustrated in Scheme 1, the notations 5′-B_1b_2-5′ and 3′-b_1B_2-3′ stand for partners in interstrand coupling. The values of J and S for identical nucleobases are much larger for GG and TT than for AA and CC. The largest intrastrand charge-transfer integral is obtained for 5′-GT-3′. In most cases the interstrand charge-transfer integrals for 5′-XY-5′ and 3′-XY-3′ are smaller than the intrastrand charge-transfer integrals involving the same nucleobases. Interestingly, the interstrand charge-transfer integrals for two adenines are significantly larger than the intrastrand charge-transfer integral, in agreement with the results in refs 36 and 72.

As has been discussed earlier,[73,81,82] dynamic disorder caused by motion of stacked base pairs along different degrees of freedom can strongly affect hole transport in DNA. It is also expected that base pair twisting makes the major contribution to this effect.[81] To include the influence of stack dynamics on hole transport in DNA hairpins, the charge-transfer and spatial overlap integrals were calculated as a function of the twist angle, θ. The values of intrastrand charge-transfer and spatial overlap integrals for identical nucleobases in neighboring base pairs are given in Figure 3. Results for all possible combinations of nucleobases are provided as Supporting Information. As follows from the data plotted in Figure 3, the values of J and S indeed exhibit a strong variation with θ, and therefore this effect cannot be ignored in studies of rate processes in DNA.

For each twist angle, the charge-transfer integrals discussed above were calculated directly as the off-diagonal matrix elements of the Kohn−Sham Hamiltonian with inverted sign. These values of J can be used in theoretical studies of hole transport in DNA, provided the spatial overlap matrix elements S are explicitly taken into account. This is done in the tight-binding calculations of charge transport discussed in the next section. By contrast, in calculations of electronic couplings for superexchange, the spatial overlap integrals are often assumed to be zero. If, however, this assumption is not valid, the electronic couplings for superexchange can be calculated using generalized charge-transfer integrals,[74]

$$J' = J - S(\epsilon_1 + \epsilon_2)/2 \qquad (3)$$

instead of J. Obviously the latter expression reduces to $J' = J - S\epsilon$ if $\epsilon_1 = \epsilon_2 = \epsilon$. The value of J' can then be obtained directly from the orbital splitting.[74]

The values of J' calculated according to eq 3 are included in Table 3. The generalized charge-transfer integrals between the nucleobases within a Watson−Crick base pair are $J' = -0.055$ eV for G:C and $J' = -0.047$ eV for A:T. In earlier studies,[36,71−73] charge-transfer integrals have been obtained by a different method based on the energetic splitting between the HOMO and HOMO−1 in a system of two nucleobases. The trends in the values of J' obtained in the present work are close to the results in refs 36, 71−73. However, some quantitative

(76) Chong, D. P.; Gritsenko, O. V.; Baerends, E. J. *J. Chem. Phys.* **2002**, *116*, 1760−1772.
(77) Lu, X.-J.; El Hassan, M. A.; Hunter, C. A. *J. Mol. Biol.* **1997**, *273*, 681−691.
(78) Sugiyama, H.; Saito, I. *J. Am. Chem. Soc.* **1996**, *118*, 7063−7068.
(79) Hush, N. S.; Cheung, A. S. *Chem. Phys. Lett.* **1975**, *34*, 11−13.
(80) Voityuk, A. A.; Jortner, J.; Bixon, M.; Rösch, N. *Chem. Phys. Lett.* **2000**, *324*, 430−434.
(81) Voityuk, A. A.; Siriwong, K.; Rösch, N. *Phys. Chem. Chem. Phys.* **2001**, *3*, 5421−5425.
(82) O'Neill, M. A.; Barton, J. K. *J. Am. Chem. Soc.* **2004**, *126*, 13234−13235.

Table 3. Charge-Transfer Integrals, J (in eV), Overlap Matrix Elements, S, and Generalized Charge-Transfer Integrals, J' (in eV), for Nucleobases Stacked at a Distance of 3.38 Å with a Twist Angle of 36°

	5′-B_1B_2-3′			3′-b_1b_2-5′			5′-B_1b_2-5′			3′-b_1B_2-3′		
	J	S	J'	J	S	J'	J	S	J'	J	S	J'
GG	0.119	0.008	0.053	0.119	0.008	0.053	0.046	0.004	0.012	−0.075	−0.005	−0.032
AA	−0.038	−0.004	−0.004	−0.038	−0.004	−0.004	0.122	0.010	0.031	0.148	0.011	0.049
CC	0.042	0.002	0.022	0.042	0.002	0.022	0.002	0.0001	0.001	0.030	0.002	0.010
TT	0.180	0.012	0.072	0.180	0.012	0.072	0.009	0.001	0.001	0.016	0.001	0.006
GA	−0.186	−0.013	−0.077	−0.013	−0.0003	−0.010	−0.048	−0.004	−0.013	−0.037	−0.003	−0.011
GC	−0.295	−0.020	−0.114	0.026	0.002	0.009	0.004	0.0002	0.002	0.059	0.004	0.022
GT	0.334	0.023	0.141	0.044	0.003	0.018	−0.018	−0.001	−0.009	−0.049	−0.003	−0.014
AC	0.091	0.005	0.042	−0.008	−0.001	−0.002	−0.004	−0.0003	−0.001	0.045	0.003	0.017
AT	−0.157	−0.010	−0.063	−0.068	−0.004	−0.031	0.035	0.003	0.007	−0.026	−0.002	−0.007
CT	−0.161	−0.011	−0.055	−0.066	−0.004	−0.028	0.0004	0.001	0.0003	−0.015	−0.002	0.004

Scheme 1

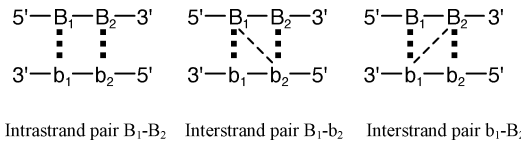

differences exist. In particular, the absolute value of J' for adenines found in the present work is 0.004 eV, while the orbital splitting procedure based on Hartree−Fock or DFT calculations yields J' ranging from 0.02 to 0.05 eV.[36,71−73]

Several factors can account for the differences between the results of the current work and the other data from the literature. For instance, the differences can arise due to the use of a much larger basis set in the present calculations. It was indeed found that a smaller basis set of double-ζ quality (DZP) and only one set of polarization functions (basis set III in ADF), with a size comparable to that of the 6-31G* basis set exploited in refs 28, 36, 72, and 83, yields a larger magnitude (0.01 eV) for the intrastrand generalized charge-transfer integral between adenines. In addition, the values of charge-transfer integrals reported earlier[36,72] were obtained by applying an electric field to bring the site energies ϵ_1 and ϵ_2 into resonance. As a consequence, the J' values calculated in the presence of a field coincide with the results obtained without a field only if $|S(\epsilon_1 - \epsilon_2)| \ll 2|J|$; otherwise they should differ by an amount equal to $S(\epsilon_1 - \epsilon_2)/2$.

Hole Dynamics and Equilibria

1. Tight-Binding Calculations of Hole-Transfer Rates. The rates of hole transfer between the G site nearest to **Sa** and the distal GG doublet in the DNA hairpins shown in Figure 1 were calculated using a quantum mechanical description of the hole combined with a classical description of the twisting motion of the base pairs. The nucleobases in the base pairs containing the proximal and distal G's and those in the intervening base pairs were included in the calculations. The other nucleobases in the DNA hairpins in Figure 1 were discarded from the calculations. Similar to previous studies of charge transfer through DNA,[42,69,84] the hole was described by the Hamiltonian in eq 1 with site energies, charge transfer, and spatial overlap integrals taken from Table 2, Figure 3, and the Supporting Information. To directly access the rate for forward hole transfer, without complications due to competition with the backward process, the charge was forced to decay irreversibly at the GG doublet by adding a complex part, $-i\hbar/\tau$, with $\tau = 100$ fs, to the site energies in this doublet.

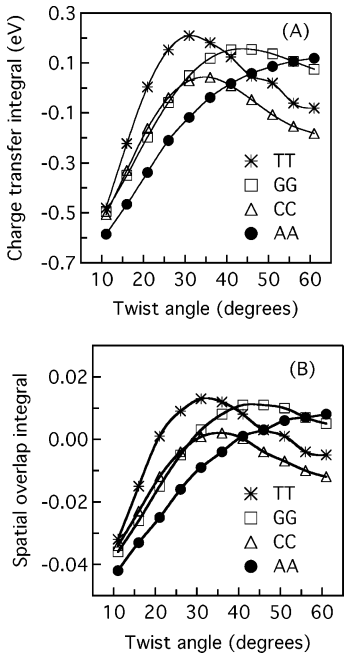

Figure 3. Charge-transfer (A) and spatial overlap (B) integrals versus the twist angle between neighboring base pairs in the same strand.

It was found that variations of twist angle and distance between base pairs have a negligible effect on the site energies. However, the twist angle strongly affects the charge-transfer integrals, as mentioned above. The dynamics of the latter degree of freedom was assumed to be harmonic and was described classically by the Hamiltonian

$$H_{\mathrm{tw}} = \frac{1}{2}\sum_m [I_m \dot{\theta}_m^{\,2} + F_{m,m+1}(\theta_{m+1}(t) - \theta_m(t) - \theta_{m,m+1}^{\mathrm{eq}})^2] \quad (4)$$

where I_m is the moment of inertia of the mth base pair, $F_{m,m+1}$ the force constant for twisting, and $\theta_{m,m+1}^{\mathrm{eq}}$ the equilibrium twist angle for the base pairs m and $m+1$. Experimental values for the force constants were taken from ref 85, and theoretical values for the equilibrium twist angles were taken from ref 86.

The wave function of the hole is expressed as a time-dependent superposition of the HOMOs on the nucleobases, i.e.,

$$\psi(t) = \sum_i c_i(t)\varphi_i \quad (5)$$

(83) Endres, R. G.; Cox, D. L.; Singh, R. R. P. *Condensed Matter* **2002**, cond-mat/021404 (http://arxiv.org/archive/cond-mat).
(84) Berlin, Y. A.; Burin, A. L.; Siebbeles, L. D. A.; Ratner, M. A. *J. Phys. Chem. A* **2001**, *105*, 5666−5678.

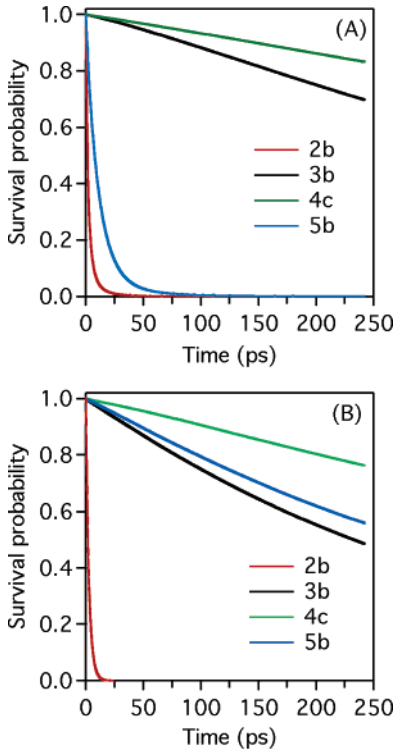

Figure 4. Probability for the hole to survive trapping at the GG doublet in hairpins shown in Figure 1 in the absence (A) and presence (B) of the Coulomb interaction.

Since initially the hole is localized on the single G site with $i = 1$, the initial condition for the wave function can be written as $c_{i=1}(t=0) = 1$ and $c_{i\neq1}(t=0) = 0$. The initial angular velocities and twist angles were sampled from a Boltzmann distribution at 293 K.

The wave function is propagated during a time step dt taken sufficiently small so that the twist angles can be considered fixed. The coefficients $c_i(t)$ are obtained numerically by integration of the first-order differential equations that follow from substituting the wave function in eq 5 into the time-dependent Schrödinger equation, which yields $i\hbar\mathbf{S}(\partial\mathbf{c}/\partial t) = \mathbf{Hc}$, with $\mathbf{c}$ the vector containing the coefficients of the HOMOs in eq 5. Note that the overlap matrix $\mathbf{S}$ is explicitly taken into account. The twist angles and angular velocities are propagated during the same time step dt by numerically solving the first-order differential equations that follow from the Hamiltonian in eq 4. This procedure is repeated until the decay of the charge is completed.

The rate of forward hole transfer between the proximal G and distal GG doublet can be obtained from the probability, $P(t)$, that a positive charge will survive trapping by GG at time t. This probability, hereafter referred to as the survival probability, is given by

$$P(t) = \sum_i |c_i(t)|^2 \qquad (6)$$

Figure 4A shows calculated time dependencies of the survival probabilities for the sequences in Figure 1. For sequences with G bases located at the same strand (sequences **2b**, **3b**, and **4c**), the forward hole transfer is seen to be fastest for the stilbene-capped hairpin **2b**. Clearly, the decay of the survival probability calculated for the other systems with the same arrangement of G bases is slower. The rate k_t of the forward hole transfer is smaller for sequence **4c** than for **3b**. These trends in the kinetics of forward hole transfer discussed above are consistent with the behavior of k_t for sequences **2b**, **3b**, and **4c** deduced from the experiments (see Table 1) and can be explained by the significantly higher site energy of T in sequence **3b** (9.111 eV) as compared to the site energy of A in sequence **2b** (8.343 eV). The rate in sequence **4c** is smaller than in **2b** due to the longer bridge consisting of two A:T base pairs separating the proximal G and the distal GG.

For the hairpin **5b**, in which G bases are located on different strands, the k_t value is significantly larger than for sequences **3b** and **4c**. This is due to the fact that the *interstrand* charge-transfer integral for 5′-AG-5′ is comparable to the J' value for *intrastrand* transfer via 5′-AG-3′ (see Table 3). Note, however, that k_t calculated for sequence **5b** disagrees with the experimental rate, which was found to fall into the range between the values obtained for hairpins **3b** and **4c**. This discrepancy is not surprising since the charge-transfer rates will be affected by the Coulomb interaction between the $\mathbf{Sa}^{-\bullet}$ anion and the hole generated in the system.

The effect of the hole interaction with $\mathbf{Sa}^{-\bullet}$ was taken into account by adding the Coulomb term with the dielectric constant 3.5 [87] to the site energies of the nucleobases. The survival probabilities calculated in the case where the Coulomb interaction is included in the calculations are shown in Figure 4B. Comparison of the data presented in Figure 4A,B shows that the Coulomb interaction leads to the increase of the rate for forward hole transfer in sequences **2b**, **3b**, and **4c**, while for sequence **5b** this rate becomes smaller. As a result, the calculated k_t values increase in the order **4c** < **5b** < **3b** < **2b**, in qualitative agreement with the trend observed for the experimental rates (see Table 1).

The effect of the Coulomb interaction on k_t is the direct consequence of changes in energetics of the charge-transfer process. In particular, for sequences **2b**, **3b**, and **4c**, the Coulomb interaction brings the site energies of the proximal G and the distal GG closer to resonance, thus enhancing the rate of charge transfer. On the basis of our calculations, the opposite situation is expected to arise for sequence **5b**. As can be seen from the data summarized in Table 2, in the absence of the Coulomb interaction between the $\mathbf{Sa}^{-\bullet}$ anion and the hole, the site energy of the proximal G (8.124 eV) is almost in resonance with that of the G at the 5′-end of the sequence (8.130 eV). The Coulomb interaction decreases the site energy of the proximal G more than that of the distal GG doublet. As a consequence, an energy gap of 0.14 eV between the G at the 5′-end and the proximal G in sequence **5b** arises. This, in turn, leads to a decrease of the rate for hole transfer.

Thus, the tight-binding calculations offer a qualitative explanation of the trend observed for the experimental rates of the forward hole transfer between proximal G and distal GG doublet in hairpins **2b**, **3b**, **4c**, and **5b**. However, the absolute values of the experimental rates are about 3 orders of magnitude smaller than those obtained from the data in Figure 4B. This

(85) Lankas, F.; Sponer, J.; Langowski, J.; Cheatham, T. E. *Biophys. J.* **2003**, *85*, 2872−2883.
(86) Olson, W. K.; Gorin, A. A.; Lu, X.-J.; Hock, L. M.; Zhurkin, V. B. *Proc. Natl. Acad. Sci. U.S.A.* **1998**, *95*, 11163−11168.
(87) Makarov, V.; Pettitt, B. M.; Feig, M. *Acc. Chem. Res.* **2002**, *35*, 376−394.

can be understood, since it is well known that an excess charge in DNA induces an internal reorganization of nucleobases and an external reorganization of the surrounding water.[36,88−91] These two processes, which have not been taken into account in the tight-binding calculations considered above, can reduce the rate of hole transfer, as discussed in the next section.

2. Superexchange Rates and Reorganization Energy. According to the standard electron-transfer theory (see, e.g., refs 46, 70, 92, and 93), the charge-induced reorganization is characterized by the so-called total reorganization energy λ. Similar to other electron-transfer reactions, λ for hole transfer in DNA can be written as a sum of two terms. These correspond to the contributions to the energetics from an internal reorganization of nucleobases and an external reorganization of the surrounding water.

If temperature T is sufficiently high that vibrational modes can be treated classically, the effect of λ on the nonadiabatic charge-transfer rate can be described theoretically using the familiar Marcus equation,[46,70,92,93]

$$k_{CT} = \frac{2\pi}{\hbar}\frac{|V_{da}|^2}{\sqrt{4\pi\lambda kT}}\exp\left(-\frac{(\Delta E_{da}+\lambda)^2}{4\lambda kT}\right) \qquad (7a)$$

where k is the Boltzmann constant, V_{da} is the electronic coupling matrix element, and ΔE_{da} is the energetic difference of the hole at the donor and acceptor sites. For superexchange charge transfer through a single bridge of n nucleobases, V_{da} is defined by

$$V_{da} = (J'_{d1}J'_{na}/\Delta E_{d,1})\prod_{k=1}^{n-1}(J'_{k,k+1}/\Delta E_{d,k+1}) \qquad (7b)$$

with J' being the generalized charge-transfer integral. In eq 7b, $\Delta E_{d,i}$ is the energetic difference of the positive charge at the hole donor (single G and GG doublet for forward and backward transfer, respectively) and the ith bridge site. The difference $\Delta E_{d,i}$ is the sum of two differences. One is the difference between the site energies of the hole at the donor and ith bridge site taken from Table 2. The other is the difference between the Coulomb interaction between the $\mathbf{Sa}^{-\bullet}$ anion and the hole on the donor and the ith bridge site. The dielectric constant was taken equal to 3.5.[87]

Equation 7 was used in the present work as a theoretical framework for numerical calculations of rates k_t and k_{-t} for forward and backward hole transfer between the proximal G and the distal GG doublet. Twisting of the base pairs was taken into account by using mean values of the charge-transfer integrals:

$$\langle|J'_{ij}|^2\rangle = \int_{\theta_{min}}^{\theta_{max}} |J'_{ij}(\theta_{ij})|^2 p(\theta_{ij})\, d\theta_{ij} \qquad (8a)$$

These values were obtained by averaging $J'_{ij}(\theta_{ij})$ over the Boltzmann distribution $p(\theta_{ij})$ of twist angles θ_{ij},

$$p(\theta_{ij}) = \exp\left(-\frac{F_{ij}(\theta_{ij}-\theta_{ij}^{eq})^2}{2kT}\right)\Big/\int_{\theta_{min}}^{\theta_{max}}\exp\left(-\frac{F_{ij}(\theta_{ij}-\theta_{ij}^{eq})^2}{2kT}\right) \qquad (8b)$$

calculated using a harmonic potential with experimental force constants F_{ij} from ref 85. The minimum θ_{min} and maximum θ_{max} angles in eq 8 were taken equal to 11° and 61°, respectively, which was found to be sufficient for convergence of the results. The effect of the Coulomb interaction between the hole on DNA and the $\mathbf{Sa}^{-\bullet}$ anion on the site energies was taken into account as described in the previous section.

It should be noted that the averaging procedure defined by eq 8 is valid in the limit of slow twisting motion in comparison with hole transport. The averaging in the opposite limit can be done as described in ref 94. In most cases, the latter procedure gives results which differ from the values of $\langle J'^2_{ij}\rangle$ obtained from eq 8 by less than 10%.[94]

The superexchange electronic coupling matrix elements for forward (V_t) and backward hole transfer (V_{-t}), calculated for the energetically most favorable pathway between the proximal G and the GG doublet in hairpins **2b**, **3b**, **4c**, and **5b**, are given in Table 1. The superexchange matrix elements for other pathways were found to be significantly smaller. The values of the total reorganization energies λ needed to reproduce the absolute values of the experimental rate constants invoking the semiclassical approach (see eq 7) are also given in Table 1. The λ values for all sequences studied are found to be close to 1 eV, in agreement with the results in refs 36, 88−91. LeBard et al.[91] have calculated a solvent reorganization energy of 0.69 eV within the framework of the molecular-based nonlocal model of solvent response (NMSR model) for the forward hole transfer in a hairpin similar in structure to sequence **2b**. This estimate, together with the internal reorganization energy of 0.65 eV obtained for guanine from DFT calculations,[36] gives $\lambda = 1.34$ eV, which does not differ too much from the total reorganization energy for sequence **2b** in Table 1. According to theoretical results reported by LeBard et al.,[91] the solvent reorganization energy increases by approximately 0.2 eV when an A:T base pair is added to the bridge between the G primary donor and the GG secondary donor. The same tendency follows from the data on the total reorganization energies for forward hole transfer presented in Table 1. More detailed comparison of λ values estimated in this work with those obtained in ref 91 requires the application of the NMSR model and theoretical methodology proposed here to hairpins of identical structure and to solvents of identical composition. Work in this direction is in progress now.

Implications for Hole Mobility and Transport Equilibria in DNA

The calculated results for the charge-transfer integrals can be used to obtain theoretical insight into the mobility of holes in DNA. This information is important for understanding the conducting properties of DNA. Estimations of the trap depths for multiple guanine-containing sites can be made using the calculated site energies. The results can be utilized to predict oxidative cleavage patterns in long sequences of DNA with several multiple guanine-containing sites. The implications of

(88) Tavernier, H. L.; Fayer, M. D. *J. Phys. Chem. B* **2000**, *104*, 11541−11550.
(89) Tong, G. S. M.; Kurnikov, I. V.; Beratan, D. N. *J. Phys. Chem. B* **2002**, *106*, 2381−2392.
(90) Siriwong, K.; Voityuk, A. A.; Newton, M. D.; Rosch, N. *J. Phys. Chem. B* **2003**, *107*, 2595−2601.
(91) LeBard, D. N.; Lilichenko, M.; Matyushov, D. V.; Berlin, Y. A.; Ratner, M. A. *J. Phys. Chem. B* **2003**, *107*, 14509−14520.
(92) Marcus, R. A.; Sutin, N. *Biochim. Biophys. Acta* **1985**, *811*, 265−322.
(93) Mikkelsen, K. V.; Ratner, M. A. *Chem. Rev.* **1987**, *87*, 113−153.
(94) Troisi, A.; Nitzan, A.; Ratner, A. *J. Chem. Phys.* **2003**, *119*, 5782−5788.

the present theoretical results for studies of these two aspects of the problem are considered in the subsequent two sections.

1. Mobility of Holes. The results of experimental studies on the conductance of DNA are still highly controversial and a large variety of possible electronic behavior has been suggested, ranging from DNA as an insulator to a superconductor; see the review in ref 28 and references therein. The experimental studies usually focus on current−voltage dependence measurements. The charge carrier mobility, μ, cannot be deduced from these measurements, since the charge carrier density is unknown. To the knowledge of the authors, the only study from which a value of the mobility for hole hopping along stacks of A:T base pairs can be deduced is that reported by Takada et al.,[95] who determined the rate constant, w, for hopping along such a stack to be 2×10^{10} s^{-1}. It also has been observed[95] that the measured charge separation yield, Φ_{cs}, decreases with the number of A:T pairs, N, as $\ln \Phi_{cs} = -\eta \ln(N)$. The slope η of this dependence deduced from experimental data was found to be equal to 1.7, in reasonable agreement with the theoretical value $\eta = 2$ predicted for the unbiased one-dimensional random walk. This suggests that the hopping frequency w reported by Takada et al.[95] can be used to estimate the low-field hole mobility μ from the relation[96] $\mu = (e/kT)w\delta^2$. Taking $w = 2 \times 10^{10}$ s^{-1} and stacking distance $\delta = 3.38$ Å, typical for B-DNA, we obtained that, for holes undergoing hopping motion between A bases, $\mu = 9 \times 10^{-4}$ cm^2 V^{-1} s^{-1}. Calculations based on a tight-binding description of holes moving along an ideally ordered stack of G:C base pairs give much higher μ values, but deviations from ideal stacking due to base pair twisting and disorder in the site energies significantly reduces the mobility.[69]

Obviously the above estimation is not applicable to the cases where polaronic effects become important. On the basis of the assumption that these effects are prevailing in DNA, Basko and Conwell theoretically estimated an upper limit for the low-field mobility of polarons along a DNA stack to be within the range $10^{-3}-10^{-2}$ cm^2 V^{-1} s^{-1}.[35,97] In a recent publication,[31] Conwell argues that, for a constant applied electric field of 5.8×10^3 V/cm, the average velocity of polarons arising from base-spacing distortion in the stack of A:T pairs should be 2×10^3 cm/s. This gives the low-field drift mobility of such polarons equal to 0.35 cm^2 V^{-1} s^{-1}.

Since in the present work we consider only hops between well-localized hole states, the mobility of a positive charge along a stack of either G:C or A:T base pairs was calculated using the hopping rate in eq 7a. The effect of base pair twisting on the mobility was taken into account by averaging the squared matrix element for electronic coupling between guanines or adenines over a Boltzmann distribution according to eq 8. Taking the reorganization energy equal to 1 eV (i.e., near the values in Table 1), the mobility of holes were calculated to be 10^{-4} and 2×10^{-5} cm^2 V^{-1} s^{-1} for stacks of G:C and A:T base pairs, respectively. A slightly different value of the reorganization energy equal to 0.63 eV must be used to reproduce the mobility of 9×10^{-4} cm^2 V^{-1} s^{-1} for holes on a stack of A:T base pairs, as deduced from the experiments by Takada et al.[95] More accurate calculations of the mobility require knowledge of the reorganization energy for the specific sequences studied in experiments on the conductance of DNA.

Table 4. Equilibrium Constant, K_{ht}, and Free Energy Change, $-\Delta G_{ht}$, for Hole Transport between the Proximal G Site and the Distal GG Doublet[a]

sequence	$K_{ht} = k_t/k_{-t}$	$-\Delta G_{ht}$ (eV)
2b	3.5	0.032
	(7.5)	(0.052)
3b	39.8	0.093
	(6.7)	(0.049)
4b	20.0	0.076
	(>0.5)	(−0.02)
5b	10.0	0.058
	(>3)	(>0.028)

[a] Data in parentheses were taken from ref 59.

2. Hole Transport Equilibria. Knowledge of rates k_t and k_{-t} for forward and backward hole transfer between the proximal G site and the distal GG doublet enables one to calculate the equilibrium constant $K_{ht} = k_t/k_{-t}$ and the free energy change $-\Delta G_{ht} = -kT \ln(K_{ht})$ for hole transfer, which provide information about the stability of a hole on a single G versus a GG doublet in the hairpins studied. Table 4 shows the values of these quantities obtained from the experimental rates in Table 1. For comparison, earlier estimations[59] of K_{ht} and ΔG_{ht} based on the values of rates k_t and k_{-t} found from the description of transient absorption kinetics in terms of two exponentials with adjustable amplitudes are also presented in the same table in parentheses.

Despite expected differences in the values of K_{ht} and ΔG_{ht} obtained by two different methods, the two sets of results allow a similar conclusion: the GG doublet in short DNA sequences serves as a shallow trap for moving holes with a depth of several kT. This conclusion strongly supports the earlier assumption[43] that a positive charge, which has reached a GG site in the process of hopping transport, will not be trapped by the guanine doublet irreversibly and therefore can be transferred over very large distances (up to several hundred angstroms) in long sequences with several GG sites. Long-range hole transport in DNA was indeed observed in experimental studies of oxidative strand cleavage in duplexes possessing double guanine-containing sites.[25]

It should be noted that the depths of GG traps following from both earlier studies[59] and the present estimations are much smaller than the difference between the ionization potential of an isolated G base and a GG doublet.[78] According to Kurnikov et al.,[98] this difference can be explained by taking solvation of trapping states into account. Indeed, inclusion of the solvation effect in calculations yields a GG trap depth $\sim 2\ kT$.[98] As has been shown by Conwell and Basko,[99] the same depth of GG traps can also be obtained without invoking solvation effects, but assuming the possibility of polaron formation in DNA.

Thus, the theoretical studies discussed above predict that the depth of GG traps has the same order of magnitude as the free energy change ΔG_{ht} obtained in the present work (see Table 4). However, earlier theoretical investigations[98,99] did not address the question of whether the depth of the GG trap is also dependent on the type of flanking nucleobases. Meanwhile, comparison of the ΔG_{ht} for sequence **2b** and **3b** given in Table

(95) Takada, T.; Kawai, K.; Cai, X.; Sugimoto, A.; Fujitsuka, M.; Majima, T. *J. Am. Chem. Soc.* **2004**, *126*, 1125−1129.
(96) Pope, M.; Swenberg, C. E. *Electronic Processes in Organic Crystals and Polymers*; Oxford University Press: Oxford, 1999.
(97) Conwell, E. M.; Basko, D. M. *Synth. Met.* **2003**, *137*, 1381−1383.
(98) Kurnikov, I. V.; Tong, G. S. M.; Madrid, M.; Beratan, D. N. *J. Phys. Chem. B* **2002**, *106*, 7−10.
(99) Conwell, E. M.; Basko, D. M. *J. Am. Chem. Soc.* **2001**, *123*, 11441−11445.

4 suggests a positive answer to this fundamental question. In particular, on the basis of the data presented in this table, one can conclude that the free energy change for sequence **2b**, in which the GG doublet is flanked by adenines, is much lower than that for sequence **3b** with the GG doublet flanked by T at the 5′-side. A similar conclusion follows from calculations exploiting the site energies in Table 2 and the charge-transfer integral for guanines forming a GG doublet. These theoretical findings are important for quantitative analysis of the efficiency and the rate of hole transport along the stacks of base pairs of various composition as well as for further investigations of elementary rate process in the interior of the double helices.

Conclusions

Site energies of a hole on a nucleobase in DNA were calculated directly as the diagonal matrix elements of the Kohn−Sham Hamiltonian for all possible combinations of flanking base pairs. The site energies were found to be strongly affected by the type of neighboring nucleobases in the triad 5′-XBY-3′ (X, B, Y = G, A, C). For some combinations of flanking nucleobases X and Y, the site energies do not reflect the hierarchy of the ionization energies of isolated nucleobases. Charge-transfer and spatial overlap integrals between the HOMOs on adjacent nucleobases were calculated as a function of the twist angle between the base pairs. These parameters were found to exhibit a strong dependence on the twist angle. The relative rates of hole transfer between guanine nucleobases separated by one or two A:T base pairs in stilbenedicarboxamide-linked DNA hairpins could be qualitatively reproduced by the tight-binding calculations, provided the Coulomb interaction between the negative charge on the stilbenedicarboxamide linker and the hole on the DNA strand is taken into account. However, the absolute values of the calculated rates were found to be several orders of magnitude higher than those observed experimentally. To reproduce the experimental values of rate constants quantitatively, effects of structural reorganization of the DNA nucleobases and the surrounding water were taken into account by using the semiclassical superexchange model for charge transfer. The experimental rates could be reproduced with reorganization energies about 1 eV, which is close to theoretical estimates reported in the literature. This value of the reorganization energy and the quantum chemical results for the charge-transfer integrals were used to estimate the charge carrier mobility along DNA stacks consisting of G:C or A:T base pairs. In addition, using the quantum chemical data including the site energies, it is demonstrated that hole transport equilibria in DNA hairpins are sensitive to the type of flanking base pairs around isolated G sites and GG doublets.

Acknowledgment. The Netherlands Organisation for Scientific Research (NWO) is acknowledged for financial support. C.F.G. and F.M.B. also thank the National Research School Combination−Catalysis (NRSC-C) for financial support. Y.A.B. and M.A.R. are grateful to the Chemistry Devision of the Office of Naval Research, the NASA URETI program, and the Department of Defense MURI and DURINT programs for support of the research. We thank many colleagues, particularly A. L. Burin, E. M. Conwell, and J. Jortner, for useful discussions.

Supporting Information Available: Numerical values of intrastrand charge-transfer and spatial overlap integrals for all possible combinations of nucleobases in neighboring base pairs with different twist angles. This material is available free of charge via the Internet at http://pubs.acs.org.

JA054257E